Contribution from the Research School of Chemistry, The Australian National University, Canberra, A.C.T., Australia, 2600, the Department of Chemistry, University of Otago, Dunedin, New Zealand, and the Chemistry Division, Department of Scientific and Industrial Research, Private Bag, Petone, New Zealand

Base-Catalyzed Condensation of a Coordinated Amine and a Nitrile To Form a Tridentate Amidine, [Co(en)(NH$_2$CH$_2$CH$_2$NC(NH$_2$)CH$_2$NH$_2$)X]$^{2+}$ (X = Cl, Br), and the Subsequent Hydrolysis of Halide

DAVID A. BUCKINGHAM,[*1] CHARLES R. CLARK, BRUCE M. FOXMAN, GRAEME J. GAINSFORD, ALAN M. SARGESON, MARK WEIN, and ANDREW ZANELLA
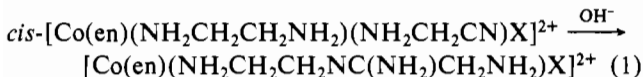
The condensation of the deprotonated amine function trans to halide in the *cis*-[Co(en)$_2$(NH$_2$CH$_2$CN)X]$^{2+}$ ions (X = Cl, Br) results in the rapid formation of the tridentate amidine [Co(NH$_2$CH$_2$CH$_2$NC(NH$_2$)CH$_2$NH$_2$)(en)X]$^{2+}$. The rate law takes the form $-d[\text{Co}]/dt = k_{Am}[\text{Co}][\text{OH}^-]$ with $k_{Am} = (9.6 \pm 0.3) \times 10^3$ mol^{-1} dm^3 s^{-1} (X = Cl), $(1.5 \pm 0.1) \times 10^4$ mol^{-1} dm^3 s^{-1} (X = Br) at 25.0 °C and $\mu = 1.0$ (NaClO$_4$), and full retention of configuration about the metal center obtains. A crystal structure of $\Lambda(+)_{546}$-[Co(NH$_2$CH$_2$CH$_2$NC(NH$_2$)CH$_2$NH$_2$)(en)Cl]Cl$_2$·H$_2$O ($P2_12_12_1$, 2811 reflections, $R = 0.049$) demonstrates a "bent" configuration of the amidine. Subsequent hydrolysis of halide follows the rate law $-d[\text{Co}]/dt = (k_1[\text{OH}^-] + k_2K[\text{OH}^-]^2)/(1 + K[\text{OH}^-])[\text{Co}]$ with $k_1 = 0.88$ mol^{-1} dm^3 s^{-1}, $k_2 = 0.14$ mol^{-1} dm^3 s^{-1}, and $K = 4.5$ mol^{-1} dm^3 (X = Cl) and $k_1 = 4.40$ mol^{-1} dm^3 s^{-1}, $k_2 = 0.90$ mol^{-1} dm^3 s^{-1}, and $K = 6.7$ mol^{-1} dm^3 (X = Br) at 25.0 °C and $\mu = 1.0$ (NaClO$_4$), where K is interpreted as the acidity constant of the amidine moiety. Two products result from each of the k_1 and k_2 paths, the first (**1**) having the same configuration as the starting complex (with full retention of optical properties) and the second (**2**) having a "planar" configuration of the amidine grouping with inversion of optical configuration about the metal. The k_1 path produces $51 \pm 2\%$ **1** and $49 \pm 3\%$ **2** and the k_2 path $70 \pm 2\%$ **1** and $30 \pm 2\%$ **2** for both X = Cl and X = Br. The structure of **2**-Cl is established by a crystal structure on [Co(NH$_2$CH$_2$CH$_2$NC(NH$_2$)CH$_2$NH$_2$)Cl]ZnCl$_4$ (*Cc*, 2131 reflections, $R = 0.049$). Strain energy minimization calculations confirm that **2** is more stable than **1** and that the remaining unobserved configurational isomer **3** is least stable. Base hydrolysis of **2**-Cl follows the rate law $-d[\text{Co}]/dt = k_2[\text{OH}^-][\text{Co}]$ with $k_2 = 26.7 \pm 0.5$ mol^{-1} dm^3 s^{-1} at 25.0 °C, $\mu = 1.0$ (NaClO$_4$); **2**-OH is the only product, and full retention of optical configuration obtains.
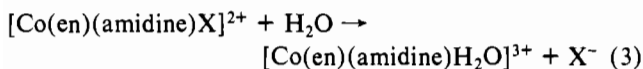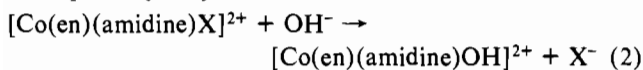
Introduction

Previously we described the formation of chelated amides via the intramolecular condensation of cobalt(III)-coordinated hydroxide (Co–OH) with the nitrile function of pendant aminoacetonitrile and aminopropionitrile where the amine is also bound to the metal (Scheme I).[2]

In this paper we discuss the related rapid formation of an amidine via the condensation of a deprotonated coordinated amine function of an ethylenediamine moiety with Co(III)-bound aminoacetonitrile, reaction 1 (X = Cl, Br), and the

$$\text{cis-[Co(en)(NH}_2\text{CH}_2\text{CH}_2\text{NH}_2)(NH}_2\text{CH}_2\text{CN)X]}^{2+} \xrightarrow{\text{OH}^-}$$
$$\text{[Co(en)(NH}_2\text{CH}_2\text{CH}_2\text{NC(NH}_2)\text{CH}_2\text{NH}_2)X]}^{2+} \quad (1)$$

subsequent hydrolysis of halide, reactions 2 and 3.

$$\text{[Co(en)(amidine)X]}^{2+} + \text{OH}^- \rightarrow$$
$$\text{[Co(en)(amidine)OH]}^{2+} + \text{X}^- \quad (2)$$

$$\text{[Co(en)(amidine)X]}^{2+} + \text{H}_2\text{O} \rightarrow$$
$$\text{[Co(en)(amidine)H}_2\text{O]}^{3+} + \text{X}^- \quad (3)$$
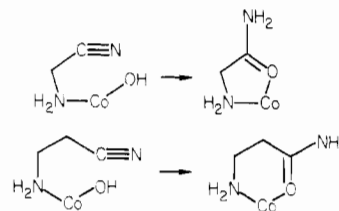
Two X-ray crystallographic analyses are used to define the condensation and base hydrolysis products, and strain energy calculations are used to relate the stabilities of the three possible isomers and to support the equilibrium data. The formation of the amidine moiety has been briefly reported in a preliminary communication.[4]

Results and Discussion

Amidine Formation. It was clear early in the investigation that an unusually fast OH$^-$-catalyzed isomerization was involved when the initial purple-red of *cis*-[Co(en)$_2$-(NH$_2$CH$_2$CN)X]$^{2+}$ (X = Cl, Br) changed to an intense

(1) To whom correspondence should be addressed at the University of Otago.
(2) (a) D. A. Buckingham, A. M. Sargeson, and A. Zanella, *J. Am. Chem. Soc.*, **94**, 8246 (1972). (b) D. A. Buckingham, P. Morris, A. M. Sargeson, and A. Zanella, *Inorg. Chem.*, **16**, 1910 (1977).
(3) Scheme I uses a shorthand notation for the two reactants *cis*-[Co-(en)$_2$(NH$_2$CH$_2$CN)(OH)]$^{2+}$ and *cis*-[Co(en)$_2$(NH$_2$CH$_2$CH$_2$CN)-(OH)]$^{2+}$ to emphasize the intramolecular nature of the condensation.
(4) D. A. Buckingham, B. M. Foxman, A. M. Sargeson, and A. Zanella, *J. Am. Chem. Soc.* **94**, 1007 (1972).

Scheme I[3]

blue-purple in slightly alkaline solution (pH 6–8).[5] This color change is quantified by the spectral changes given in Figure 1. pH stat measurements showed that, while the process is OH$^-$ catalyzed, no OH$^-$ is consumed. Infrared measurements showed the loss of the –C≡N stretching frequency at ~2370 cm^{-1} and the concomitant formation of a strong absorption at ~1660 cm^{-1}. ^{1}H NMR experiments in H$_2$O buffers also showed the appearance of a very low-field N–H signal (two protons) at ~8 ppm. Halide was not released since little or not precipitate was obtained in the presence of Ag$^+$ when the final solution was acidified. This information is consistent with the condensation of a deprotonated amine with the nitrile carbon to form a tridentate amidine ligand without the loss of halide (reaction 1).

Three possible amine functions could be involved leading to the three configurations shown in Scheme II. We preferred the amine leading to the "planar" tridentate complex **2**-X since this is the most stable and least strained configuration (see below). However, an X-ray structure determination of the chloro complex (Figure 2) identified the product as having the **1**-Cl configuration.

Ion-exchange chromatography confirmed that at least 98% of the product has this structure; no **2**-X (<2%) could be detected even when large amounts of reactant were used. It was subsequently shown that **2**-X (X = Cl, Br, OH) could be readily separated from **1**-X on Sephadex or Dowex cation

(5) At about this time we found a report that attributed the isomerization to a change from Co–NH$_2$CH$_2$CN to Co–NCCH$_2$NH$_2$ coordination with concomitant cis → trans rearrangement: S. C. Chan and F. K. Chan, *Aust. J. Chem.*, **23**, 1175 (1970).

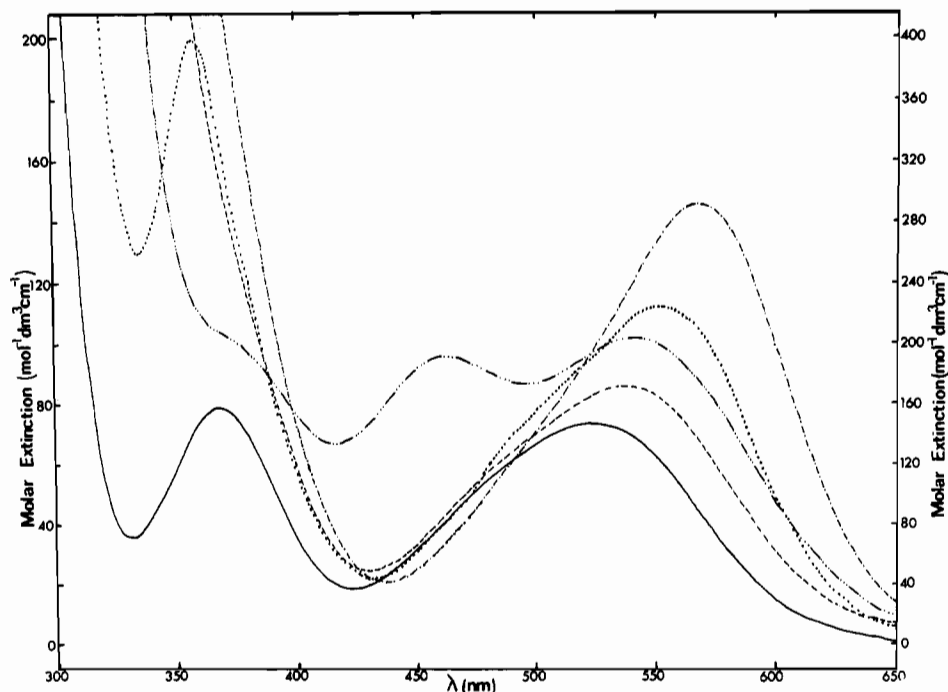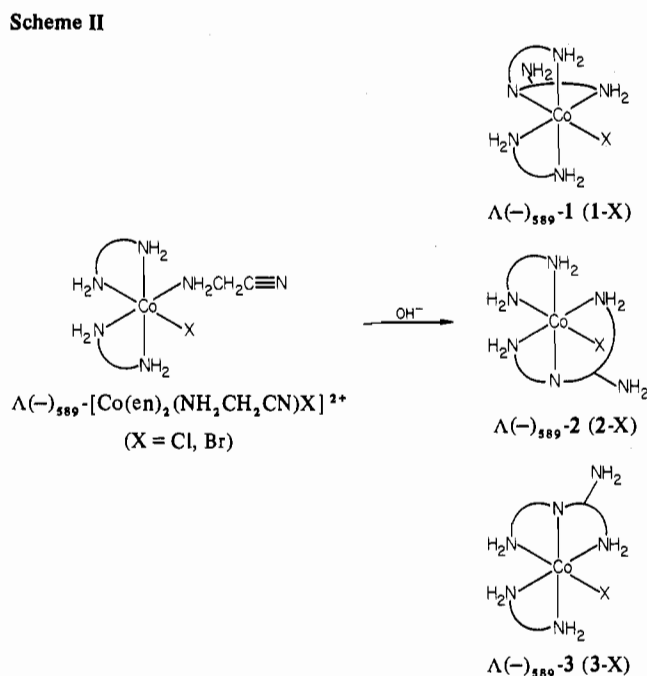**Figure 1.** Visible absorption spectra for (left-hand scale) *cis*-[Co(en)$_2$(NH$_2$CH$_2$CN)Cl]Cl$_2$ (—), *cis*-[Co(en)$_2$(NH$_2$CH$_2$CN)Br]Br$_2$ (‐‐‐), and **2**-Cl (‐·‐·‐) and (right-hand scale) **1**-Cl (···) **1**-Br (····) in 0.016 mol dm^{-3} HClO$_4$.

Scheme II

Figure 2. X-ray absolute configuration of $\Lambda(-)_{589}$-**1**-Cl.

ion-exchange resin. Also, the optical properties of $\Lambda(-)_{589}$-[Co(en)(amidine)X](ClO$_4$)$_2$ isolated following treatment of optically pure $\Lambda(-)_{589}$-[Co(en)$_2$(NH$_2$CH$_2$CN)X]$^{2+}$ ([M]$_{589}$ = -160 (X = Cl), -610° mol^{-1} cm dm (X = Br); [M]$_{436}$ = 1200 (X = Cl), 1320° mol^{-1} cm dm (X = Br))[2a] at pH 7.5 (pH stat control) agreed within 2% with those found in solution before isolation. The rotations for the isolated chloro complex also agreed with separately resolved $\Lambda(-)_{589}$-[Co(en)(amidine)Cl]Cl$_2$·H$_2$O ([M]$_{589}$ = -2450, [M]$_{546}$ = 5200, [M]$_{436}$ = 5100° mol^{-1} cm dm). However, in the absence of information concerning the properties of **3**-Cl, which has not been observed at any stage in this investigation, the possibility of traces of this isomer occurring in the condensation product cannot be completely ruled out.

Figure 3 gives the ^{1}H NMR spectrum of **1**-Cl in Me$_2$SO-*d$_6$* and Figure 4 the rotatory dispersion (RD) curve for Λ-

$(-)_{589}$-**1**-Cl. The ^{1}H NMR spectrum clearly shows an amine absorption at very low field (8.4 ppm) compared to that for the amine absorptions in [Co(en)$_2$(NH$_2$CH$_2$CN)Cl]$^{2+}$, and this absorption integrates for two protons. This agrees with both H atoms being located on the same exo-N center, and the X-ray results given below support this observation.

Isomer **1**-Cl is significantly strained in that the ethylenediamine fragment of the tridentate ligand is substantially in the envelope conformation
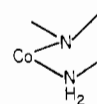
and the sp^2 N and C centers, which would prefer to be planar, are forced to have pronounced trigonal-pyramidal character
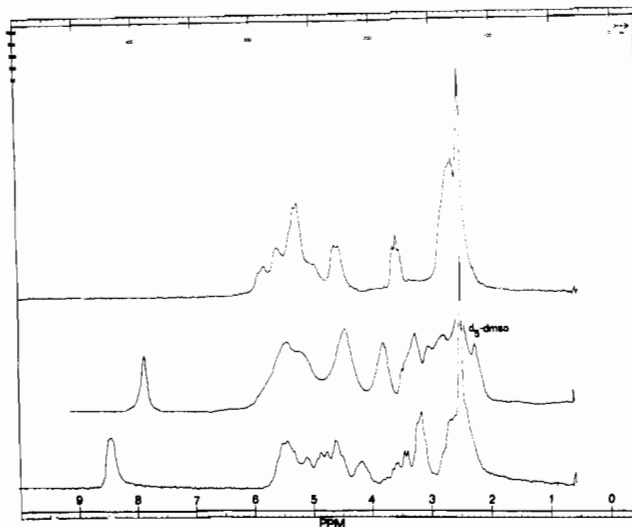
Figure 3. ^{1}H NMR spectra (100 MHz) in Me$_2$SO-d_6 of (top to bottom) *cis*-[Co(en)$_2$(NH$_2$CH$_2$CN)Cl]Cl$_2$, **2**-Cl, and **1**-Cl. The low-field signal ($\sim$8 ppm, two protons) characterizes the protons of the amidine group.

Figure 4. Rotatory dispersion curves: (a) $\Lambda(-)_{589}$-**1**-Cl (—); (b) $\Lambda(-)_{589}$-**1**-OH$_2$(- - -); (c) $\Lambda(-)_{589}$-**1**-OH ($\cdots$); (d) $\Delta(+)_{589}$-**2**-Cl (- $\cdot$ - $\cdot$); (e) $\Delta(+)_{589}$-**2**-OH (- $\cdots$ -). Treatment of (a) with OH$^-$ gives rise to (c) and (e), and treatment with Hg^{2+} gives rise to (b).

by coordination of the tridentate ligand onto a face of the octahedral ion.

An explanation for the dominance of this isomer comes from a consideration of the relative acidities of the N protons. For halopentaamine complexes of this type the amine center trans to halide exchanges $\sim$100 times faster than the amin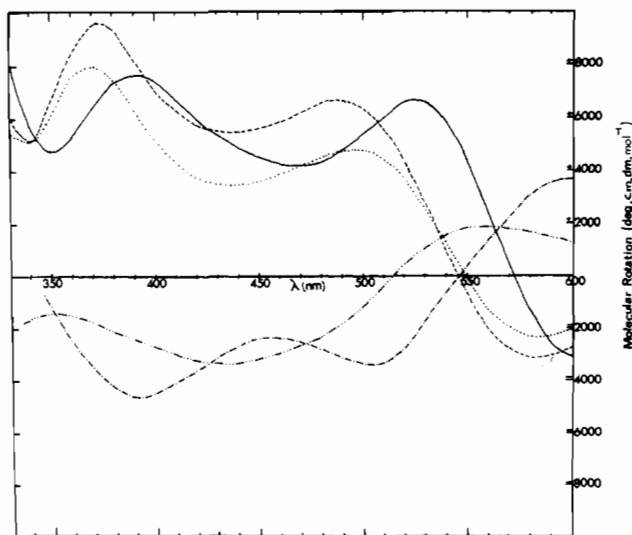e centers cis to halide.[6] If this property is taken as an index of relative acidity, then the relative abundance of the deprotonated amine centers cis and trans to halide in the *cis*-[Co(en)(en-H)-(NH$_2$CH$_2$CN)X]$^+$ species would account for the preponderance of **1**-X provided the centers had similar reactivities.

Rate data for amidine formation are given in Table I, and the simple rate law

$$-d[\text{Co}]/dt = k_{\text{Am}}[\text{Co}][\text{OH}^-] \qquad (4)$$

is followed over a 50-fold change in [OH$^-$] with $k_{\text{Am}} = (9.6 \pm 0.3) \times 10^3$ mol^{-1} dm^3 s^{-1} for X = Cl and $(1.5 \pm 0.1) \times 10^4$ mol^{-1} dm^3 s^{-1} for X = Br at 25.0 °C and $\mu = 1.0$ (NaClO$_4$). A ^{1}H NMR study in D$_2$O showed that exchange of the NH$_2$

(6) D. A. Buckingham, P. A. Marzilli, and A. M. Sargeson, *Inorg. Chem.*, **8**, 1595 (1969).

Table I. Rate Data for OH$^-$-Catalyzed Cyclization of [Co(en)$_2$(NH$_2$CH$_2$CN)X]$^{2+}$ to [Co(en)(amidine)X]$^{2+}$ at 25 °C and $\mu = 1.0$ (NaClO$_4$)^a

	X = Cl		X = Br	
10^6 [OH$^-$],^{b} mol dm^{-3}	$10^2 k_{\text{obsd}}$, s^{-1}	$10^{-3} k_{\text{Am}}$,^{e} mol^{-1} dm^3 s^{-1}	$10^2 k_{\text{obsd}}$, s^{-1}	$10^{-3} k_{\text{Am}}$,^{e} mol^{-1} dm^3 s^{-1}
0.347	0.321^d	9.3	0.496	14.3
0.901			1.28	14.2
0.935	0.920^d	9.8		
2.14	2.18^d	10.2	3.26	15.2
8.14	7.80^d	9.6	11.8	14.5
14.79	13.6^d	9.2	20.1	13.6
2.14			3.47^c	16.2
2.14			3.63^d	17.0

^{a} Spectrophotometric data with Tris–HClO$_4$ buffers (0.025 mol dm^{-3}). [complex] = 2 × 10^{-3} mol dm^{-3}. Data collected at 565, 500, 600, and 610 nm. ^{b} Calculated with use of $K_w = 1.73 \times 10^{-14}$.[16] ^{c} Buffer lowered to 0.013 mol dm^{-3}. ^{d} [complex] = 4 × 10^{-3} mol dm^{-3}. ^{e} $k_{\text{Am}} = k_{\text{obsd}}/[\text{OH}^-]$.

Scheme III
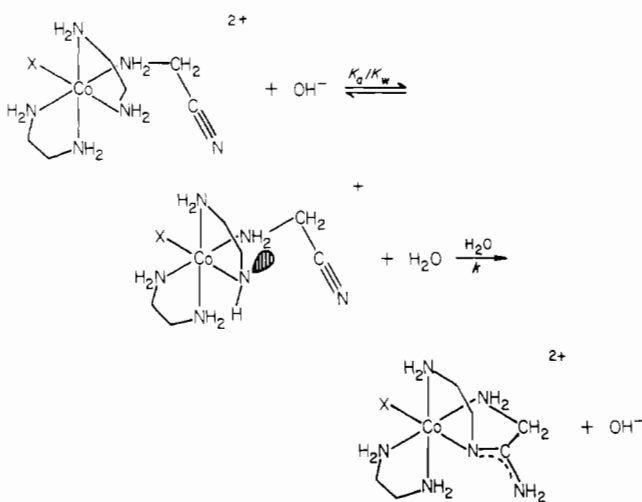
protons trans to Cl was at least 40 times faster than the cyclization process, and this agrees with proton-exchange studies on related chloropentaamine complexes where cis protons typically have rate constants of $\sim$10^4 mol^{-1} dm^3 s^{-1} and trans protons $\sim$10^6 mol^{-1} dm^3 s^{-1} at 25 °C.[6]

Another surprising feature is the rapidity of the attack of the amine at the nitrile, $k_{\text{Am}} \approx 10^4$ mol^{-1} dm^3 s^{-1}. Scheme III depicts the proposed mechanism in terms of nucleophilic attack by the deprotonated amine center trans to X at the nitrile carbon atom; this proposal gives $k_{\text{Am}} = kK_a/K_w$. For most Co(III) amine complexes pK_a values appear to be in the vicinity of 14–17 and a reasonable estimate appears to be $\sim$16 for such 2+ ions.[7] Thus $k \approx 10^6$ s^{-1}, which is surprisingly fast. It exceeds the expected rate of inversion of the deprotonated amine center[8] by a factor of 10^2–10^3. Moreover, the condensation of amines with nitriles does not appear to occur in the absence of the metal ion, i.e., in purely organic systems, at least under such mild conditions.

In summary then, this reaction, leading to the formation of the strained tridentate ring system, is directed in a regiospecific manner by the most acidic amine center that is trans to the halide moiety. It is an excellent example of a kinetically controlled reaction leading to a thermodynamically unstable product.

(7) D. A. Buckingham, C. R. Clark, and T. W. Lewis, *Inorg. Chem.*, **18**, 2041 (1979).
(8) B. Halpern, A. M. Sargeson, and K. R. Turnbull, *J. Am. Chem. Soc.*, **88**, 4630 (1966).

Table II. Rate Data for Base Hydrolysis of [Co(en)(amidine)X]$^{2+}$ (Isomer 1) to [Co(en)(amidine)OH]$^{2+}$ at 25.0 °C and $\mu = 1.0$ (NaClO$_4$)^a

	X = Cl		X = Br	
10^3[OH$^-$],^{c} mol dm^{-3}	$10^3 k_{obsd}$, s^{-1}	k_{OH},^{g} mol^{-1} dm^3 s^{-1}	$10^3 k_{obsd}$, s^{-1}	k_{OH},^{g} mol^{-1} dm^3 s^{-1}
5	4.55	0.91	23.1	4.62
10	8.80	0.88	42.7	4.27
25	22	0.88	101	4.04
50	38	0.76	177	3.54
100	69	0.69	300	3.00
150	96	0.64	418	2.79
200	125	0.62	508	2.54
250	145	0.58	600	2.40
300	164	0.55	655	2.18
350	166	0.47	721	2.06
400	171	0.43	721	1.80
450	161	0.36	801	1.78
500	184	0.37	838	1.68
600	196	0.33		
700	205	0.29	924	1.32
800	233	0.29	1120	1.40
900	250	0.28		
1000	282	0.28	1360	1.36
2^b			8.7	4.35
5^{b,e}			18	3.60
10^{b,e}	8.1	0.81	38	3.80
25^{b,f}	18.1	0.72	89	3.56
50^{b,f}	34.1	0.68	107	3.54
125^b			430	3.44
200^b			600	3.00
250^{b,d}	119	0.48		
300^b			700	2.33
400^b			880	2.20
500^{b,d}	184	0.37	1100	2.20
750^{b,d}	221	0.29		
1000^{b,d}	264	0.26		

^{a} Spectrophotometric data: $\lambda = 550$ nm (X = Cl), 450–625 nm (X = Br); [Co] = 1 × 10^{-3} mol dm^{-3} (X = Cl), 1.3 × 10^{-4} mol dm^{-3} (X = Br). ^{b} With [Co(en)$_2$(NH$_2$CH$_2$CN)X]X$_2$ as reactant. ^{c} Made up with freshly prepared 2.0 mol dm^{-3} NaOH solution. ^{d} [Co] = 4 × 10^{-3} mol dm^{-3}. ^{e} [Co] = 2.5 × 10^{-4} mol dm^{-3}. ^{f} [Co] = 2.0 × 10^{-3} mol dm^{-3}. ^{g} $k_{OH} = k_{obsd}/[OH^-]$.

Base Hydrolysis of the Halo–Amidine Complex. At higher pH base hydrolysis of X (Cl, Br) ensues, and pH stat results demonstrated that 1 mol of OH$^-$ is consumed per mole of [Co(en)(amidine)X]$^{2+}$. The intense blue is replaced by a red-purple solution and by a reduced absorption in the visible region (Figure 6).

Rate data for this process, reaction 2, are given in Table II, and a plot of k_{obsd} vs. [OH$^-$] is given in Figure 5. It is clear that a complex rate law is involved. At pH <13 the process follows a first-order [OH$^-$] dependence, but between 0.1 and 1.0 mol dm^{-3} OH$^-$ a discontinuity occurs, which emerges as a second process, also first order in OH$^-$, but some 5–6 times slower than before. The rate expression

$$k_{obsd} = \frac{k_1^1[OH^-] + k_2^1 K[OH^-]^2}{1 + K[OH^-]} \quad (5)$$

fits the data (cf. Figure 5) with k_1^1 controlling the reaction below 0.1 mol dm^{-3} OH$^-$ and k_2^1 being dominant in 1.0 mol dm^{-3} alkali. For X = Cl, $k_1^1 = 0.88$ mol^{-1} dm^3 s^{-1}, $k_2^1 = 0.14$ mol^{-1} dm^3 s^{-1}, and $K = 4.5$ mol^{-1} dm^3, and for X = Br, $k_1^1 = 4.40$ mol^{-1} dm^3 s^{-1}, $k_2^1 = 0.90$ mol^{-1} dm^3 s^{-1}, and $K = 6.7$ mol^{-1} dm^3. These k_1^1 and k_2^1 values are in the normal range expected for 2+ and 1+ halo complexes.[9]

The rate law implies deprotonation of the complex in strongly alkaline solution with both the protonated and the
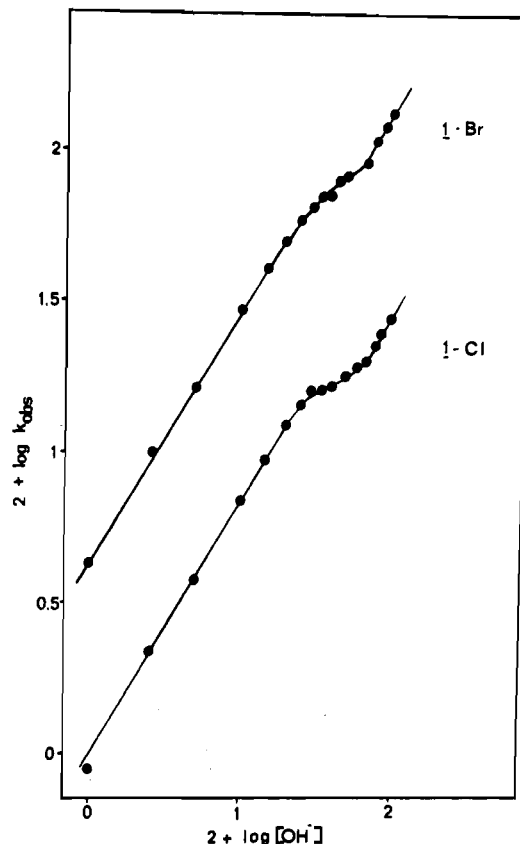
Figure 5. Plot of k_{obsd} vs. [OH$^-$] for base hydrolysis of 1-Cl and 1-Br at 25.0 °C and $I = 1.0$ (NaClO$_4$). The discontinuity occurs in the vicinity of the pK_a of the amidine group.

Scheme IV
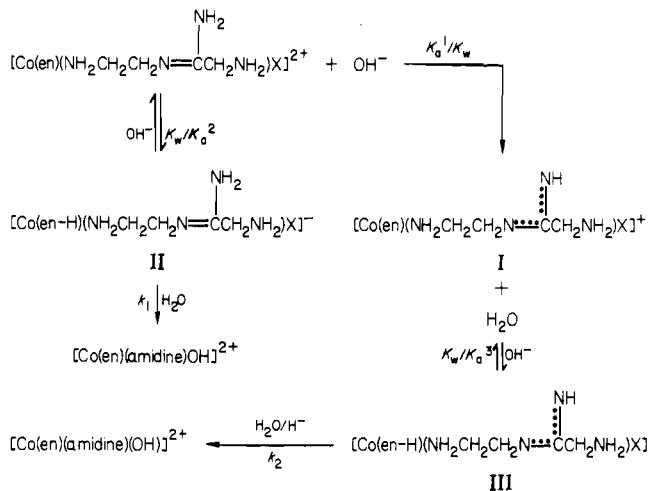
conjugate base forms undergoing OH$^-$-assisted hydrolysis. Experiments with a rapid-scan spectrophotometer attached to a stopped-flow mixing device gave clear evidence for a strongly absorbing species in 0.5 mol dm^{-3} OH$^-$ ($\lambda_{max} \approx 550$ nm for X = Cl),[10] and the deprotonated species could clearly be seen by eye in test-tube experiments as a transient greenish coloration.

The most obvious choice for deprotonation under these conditions (0.1–1.0 mol dm^{-3} OH$^-$) is the exo amidine-NH$_2$ group since the other amine centers would be expected to have pK_a values in excess of 14. Scheme IV outlines a mechanism whereby both forms of the reactant undergo the normal dis-

(9) J. O. Edwards, F. Monacelli, and G. Ortaggi, *Inorg. Chim. Acta*, **11**, 47 (1974).
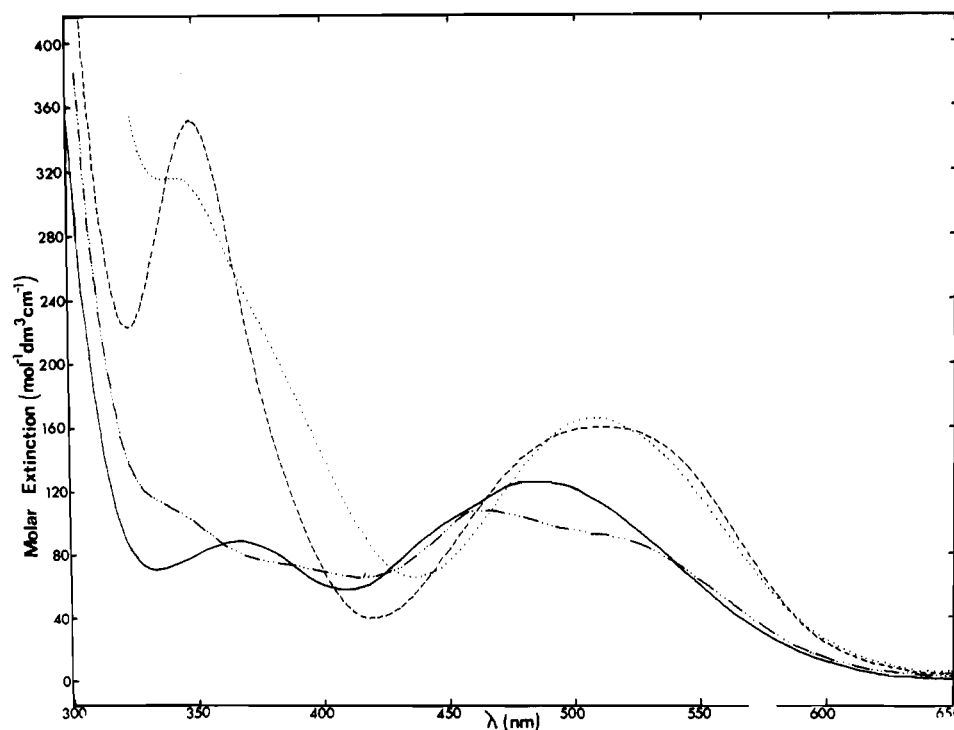
Figure 6. Visible absorption spectra for 1-H$_2$O (- - -), 1-OH (···), 2-H$_2$O (-····-), and 2-OH (—) in 10^{-3} mol dm^{-3} HClO$_4$ or phosphate buffer (pH 9.2).

sociative process through an ethylenediamine conjugate base to give hydroxo products. Evidence for the conjugate base mechanisms comes from competition studies with N$_3^-$ and NO$_2^-$, and qualitative experiments showed that both anions are readily captured. This scheme agrees with the observed data (eq 5) with $k_1^1 = k_1 K_a^2/K_w$, $k_2^1 = k_2 K_a^3/K_w$, and $K = K_a^1/K_w$ (pK_a^1(Cl) = 13.35, pK_a^1(Br) = 13.7). New features here are the apparent absence of an aquation path for the reactant deprotonated at the trans-*exo*-amidine function (I), and for deprotonation of a cis-amine function leading to hydrolysis products. Previously we had proposed deprotonation of an amine function trans to X (most acidic) as the normal route to base hydrolysis.[11] However, in view of the somewhat smaller second-order rate constants k_1 for [Co(en)(amidine)X]$^{2+}$ compared to those for related halo–pentaamine complexes (for example, for cis-[Co(en)$_2$NH$_3$X]$^{2+}$ k = 35 mol^{-1} dm^3 s^{-1} (X = Br), k = 8 mol^{-1} dm^3 s^{-1} (X = Cl)) it seems appropriate to ascribe k_1 to aquation of II with deprotonation of the cis-amine function being in the normal range expected for other complexes (pK_a ≈ 16^7). Thus amidine deprotonation, while being responsible for the discontinuity in the k_{obsd} vs. [OH$^-$] rate profile, does not lead directly to base hydrolysis products in this scheme. This is in accord with a previous proposal[12,13] that cis deprotonation, while being less efficient in an equilibrium sense (i.e., less acidic), is the preferred route to the base hydrolysis of halo(amine)cobalt(III) species.

Alternatively, k_1 could be interpreted in terms of aquation of the deprotonated reactant I, viz.

$$[Co(en)(NH_2CH_2CH_2N\overset{NH}{\underset{\cdots\cdots}{=\!=\!=}}CCH_2NH_2)X]^+$$

I

$$k_1^*\diagup \quad [OH^-]\diagdown k_2^1$$
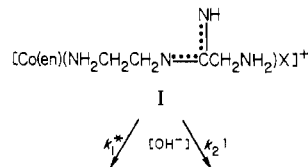
whence $k_1^* = k_1^1/K = 0.2$ s^{-1} for X = Cl. Then the ratio

$k_2^1/k_1^* ≈ 1.0$ mol^{-1} dm^3 becomes unusually low compared to that normally encountered for base hydrolysis and aquation processes (viz., 2 × 10^7 for cis-[Co(en)$_2$NH$_3$Cl]$^{2+}$).[9] But k_1^* would represent aquation of the amido species, and this may well be unusually fast. Hence, a clear distinction between the above alternative mechanisms cannot be made at this time.

Treatment of the hydroxy products with HCl or HBr leads to regeneration of the [Co(en)(amidine)X]$^{2+}$ ions. Chromatography of these on Na$^+$ Dowex or Sephadex ion-exchange resins resulted in the separation of two bands with the faster moving red product having the same absorption spectrum (Figure 6) and RD curve (Figure 4) as the reactant, and the slower moving orange product having significantly different visible (Figure 6) and RD (Figure 4) properties. The formation of two [Co(en)(amidine)X]$^{2+}$ isomers[14] was confirmed with use of larger amounts of material, and both ions were isolated and characterized as the [Co(en)(amidine)X]Cl(ClO$_4$) or [Co(en)(amidine)X]ZnCl$_4$ species. The absence of any isomerization during the treatment with HCl or HBr was verified by similarly treating the pure isomeric [Co(en)(amidine)(H$_2$O)]$^{3+}$ ions generated by the Hg^{2+}-induced removal of halide (see below); the anation process preserves both the configuration and the optical purity of the aqua ions. Other experiments demonstrated that both the aqua and the hydroxy ions were stable to configurational change over the times necessary for carrying out the experiments.

The RD results starting with optically pure Λ(−)$_{589}$[Co(en)(amidine)Cl]$^{2+}$ (Λ-1-Cl) are given in Figure 4 and are summarized by eq 6. Clearly the two products have catoptric configurations about the metal center.

The planar geometry of the tridentate amidine ligand was established by an X-ray investigation of a racemic crystal of **2**, [Co(en)(amidine)Cl]ZnCl$_4$ (Figure 7), isolated following similar treatment of 2-OH with HCl.

A proposal for the origin of the two products is depicted in Scheme V. The five-coordinate intermediate generated by

(11) A. M. Sargeson, *Pure Appl. Chem.*, **33**, 527 (1973).
(12) F. R. Nordmeyer, *Inorg. Chem.*, **8**, 2780 (1969).
(13) C. K. Poon, *Inorg. Chim. Acta, Rev.*, **4**, 123 (1970).

(14) In a previous paper by K. B. Nolan and R. W. Hay, *J. Chem. Soc., Dalton Trans.*, 914 (1974), it was reported that this reaction gave stereoretentive products only.

$[M]_{436} = 5240°$

$$+ \; OH^- \longrightarrow$$

$[M]_{436} = 3480°$ $[M]_{436} = -3380°$

| HCl | HCl

$[M]_{436} = 5050°$ $[M]_{436} = -2820°$ (6)

Figure 7. X-ray structure of 2-Cl^{2+} cation (note that the crystal is racemic).
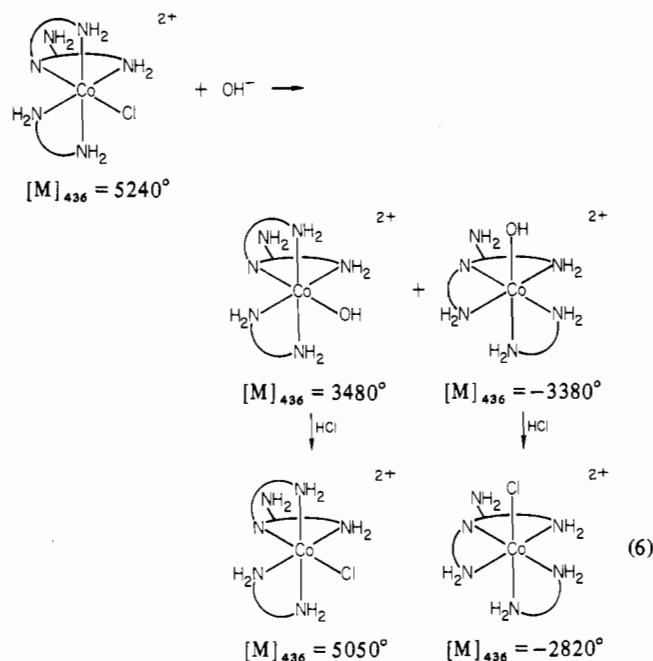
loss of X either aquates without stereochemical change (path a) or the entry of water accompanies two concerted edge displacements (path b), encouraged by the driving force for the planar condition of the amidine N atom bound to the metal. As we will see below, this planar condition is the thermodynamically favored form, but it appears that entry of H$_2$O into the five-coordinate intermediate is sufficiently fast to trap some of the reactant in its original configuration. It is not known yet whether this process involves competitive entry into a single distorted intermediate (as shown) or whether the initially formed symmetrical form reacts with water and competitively rearranges to the more stable planar condition.

The distribution between the two isomeric products also shows interesting trends. Table III lists these as a function of leaving group (X = Cl, Br) and OH$^-$ concentration. Within experimental error ($\pm2\%$) the distribution is the same for the two leaving groups, and this is consistent with other investigations of the type, i.e., for base hydrolysis of the $(+)_{589}$-$[Co(en)_2(NH_3)X]^{2+}$ ions, X = Cl$^-$, Br$^-$, NO$_3^-$.[15] More interestingly, however, the product distribution varies with OH$^-$, with the percentage of **1-OH** being at a maximum of $\sim70\%$ in 1.0 mol dm^{-3} OH$^-$ but dropping off rapidly to $\sim57\%$ in 0.1 mol dm^{-3} OH$^-$ and to 51% in 6.8×10^{-4} mol dm^{-3} OH$^-$. Qualitatively this variation follows the change in reactant from the deprotonated amidine species [Co(en)(amidine-H)X]$^+$ to its conjugate acid [Co(en)(amidine)X]$^{2+}$ with the product distribution from the former being 70 $\pm$ 2% **1-OH**, 30 $\pm$ 2% **2-OH**, and the latter being 51 $\pm$ 2% **1-OH**, 49 $\pm$ 3% **2-OH**. In terms of Scheme V this implies a reduced ability for rearrangement in the intermediate arising from [Co(en)(amidine-H)X]$^+$ to form the "planar" tridentate (path b), possibly as a result of the enhanced delocalization of negative charge in the N$\cdots$C$\cdots$NH grouping of the amidine.

Base Hydrolysis and Aquation of 2-Cl. Unlike **1-Cl**, the "planar" [Co(en)(amidine)Cl]$^{2+}$ isomer does not show a discontinuity in the rate law

$$k_{obsd} = k_{OH}^{II}[OH^-] \qquad (7)$$

for base hydrolysis, at least up to [OH$^-$] = 1.0 mol dm^{-3} (Table
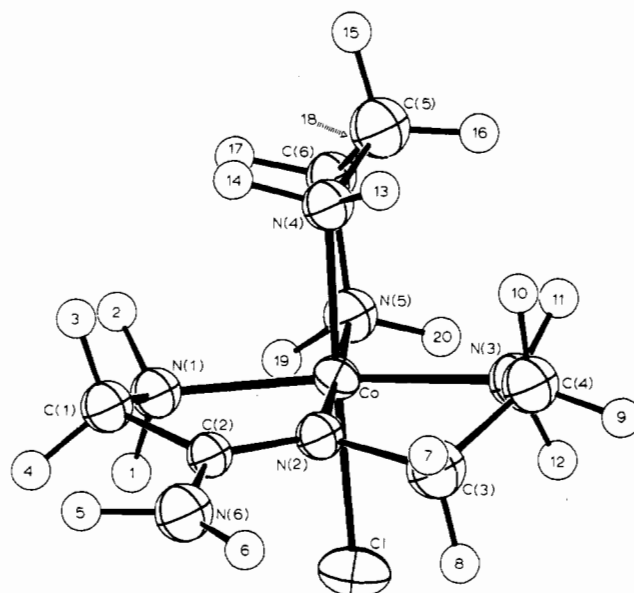
Table III. Percentage Product Distribution from the Base Hydrolysis of [Co(en)amidineX]$^{2+}$ Ions at 25 °C and $\mu = 1.0$[a]

[NaOH], mol dm^{-3}	1-Br		1-Cl		2-Cl	
	1-OH	2-OH	1-OH	2-OH	1-OH	2-OH
1.0	69.4,	30.6,	68.6,	31.4,	...	99.3
	71.7	28.3	65.6	34.4		
0.4	61.9	38.1	60.4	39.6		
0.2	58.5	41.2	55.7	44.3		
0.1	57.3	42.7	55.4	44.6	...	99.6
0.05			55.6	44.4		
4.3×10^{-3}	53.5	46.5				
1.7×10^{-3}	51.5	48.5				
6.8×10^{-4}	52.0	48.0				

[a] Estimated as aquo ions (350 nm) following HClO$_4$ quenching of reaction mixtures after $(20-30)t_{1/2}$; ϵ_{350} 351 (1-OH$_2$), 83.6 (2-OH$_2$). Identical product distributions were found after separating 1-OH$_2$ and 2-OH$_2$ chromatographically (Sephadex SP-C25, eluant 0.1 mol dm^{-3} NaH$_2$PO$_4$/NaH$_2$PO$_4$) and separately estimating 1-OH$_2$ at 514 nm (λ_{max}; ϵ_{max} 159) and 2-OH$_2$ at 460 nm (λ_{max}; ϵ_{max} 108.5). Aquo spectra were obtained from Hg^{2+}-induced aquation of the corresponding 1-Cl, 1-Br, and 2-Cl amidine complexes.

Table IV. Rate Data[a] for Base Hydrolysis of [Co(en)(amidine)Cl]Cl·ClO$_4$ (2-Cl) to [Co(en)(amidine)OH]$^{2+}$ at 25 °C and $\mu = 1.0$ (NaClO$_4$)

[NaOH], mol dm^{-3}	k_{obsd}, s^{-1}	k_{OH},[b] mol^{-1} dm^3 s^{-1}	[NaOH], mol dm^{-3}	k_{obsd}, s^{-1}	k_{OH},[b] mol^{-1} dm^3 s^{-1}
0.01	0.267	26.7	0.2	5.24	26.3
0.02	0.524	26.2	0.3	7.95	26.5
0.05	1.37	27.5	0.4	10.5	26.3
0.07	1.87	26.7	0.5	13.3	26.6
0.1	2.63	26.3	1.0	27.8	27.8

[a] Spectrophotometric data: $\lambda = 600$, 480 nm; [complex] = 1.2×10^{-3} mol dm^{-3}. [b] $k_{OH} = k_{obsd}/[OH^-]$.

Table V. Rate Constants for Aquation of 1-Cl·Cl·ClO$_4$ at 25 °C and $\mu = 1.0$ mol dm^{-3} (NaClO$_4$)[a]

[HClO$_4$], mol dm^{-3}	$10^4 k_{obsd}$, s^{-1}	[HClO$_4$], mol dm^{-3}	$10^4 k_{obsd}$, s^{-1}
0.1	2.28	1.0	2.14
0.5	2.24		

[a] [Co]$_T$ = 5×10^{-3} mol dm^{-3}; $\lambda = 550$ nm.

(15) D. A. Buckingham, I. I. Olsen, and A. M. Sargeson, *J. Am. Chem. Soc.*, **90**, 6654 (1968).

(16) H. S. Harned and W. J. Hamer, *J. Am. Chem. Soc.*, **55**, 2194 (1933). A more recent value of pK_w in 1.0 mol dm^{-3} NaClO$_4$ (13.80) agrees closely with this: R. Fischer and J. Bye, *Bull. Soc. Chim. Fr.*, 2920 (1964).

Scheme V

Λ-1-X

Λ-1-OH Λ-2-OH
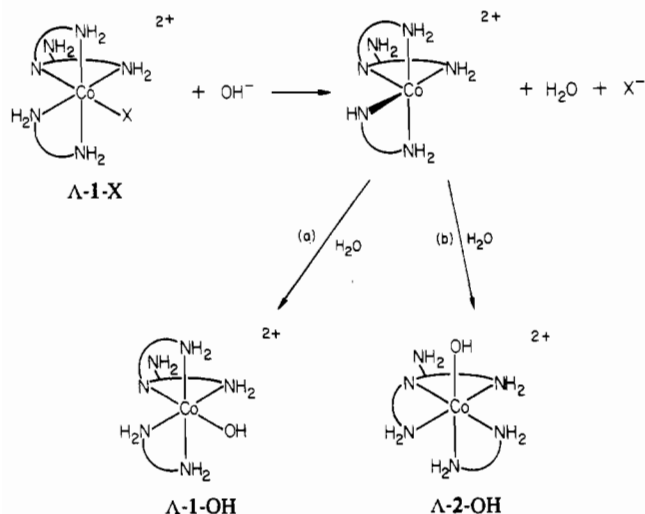
IV). The second-order rate constant, $k_{OH} = 26.7 \pm 0.5$ mol^{-1} dm^3 s^{-1}, is some 30 times larger than that for **1-Cl**, but it is not clear yet whether this results from an enhanced acidity of an amine proton or from the greater reactivity of the conjugate base toward loss of Cl$^-$. What is clear is that the planar amidine grouping in this isomer, with an otherwise unaltered disposition of the ligands about the metal, is less acidic than in **1-Cl** with the pK_a now lying somewhat above 14. If the cis amidine proton is responsible for hydrolysis in **2-Cl**, these rate and acidity comparisons lend further weight to the argument given above for the amidine moiety not being responsible for hydrolysis in **1-X**.

Again, unlike the case for isomer **1**, the products of base hydrolysis are straightforward with only **2-OH** being formed at all pHs. This was shown by ion-exchange analysis of both the immediate hydroxo product and the chloro product following anation with HCl. Furthermore, full retention of chirality obtains in this process (eq 8). Δ-**2-Cl**$^{2+}$ also aquated

$$\Delta\text{-}2\text{-}Cl^{2+} + OH^- \xrightarrow{} \Delta\text{-}2\text{-}OH^{2+} + Cl^- \xrightarrow{HCl}$$
$$[M]_{589} = \qquad\qquad [M]_{589} =$$
$$5500° \qquad\qquad 1460°$$
$$\Delta\text{-}2\text{-}Cl^{2+} + H_2O \quad (8)$$
$$[M]_{589} =$$
$$5380°$$

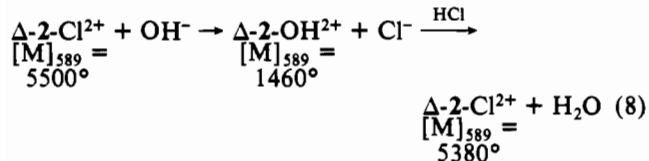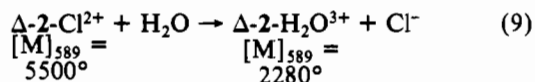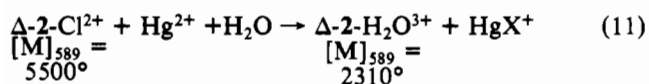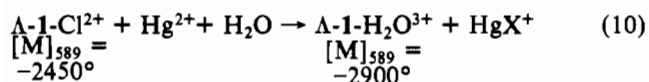slowly in acid solution (Table V) to form Δ-**2-H$_2$O**$^{3+}$ again with full retention of configuration and chirality (eq 9). The

$$\Delta\text{-}2\text{-}Cl^{2+} + H_2O \rightarrow \Delta\text{-}2\text{-}H_2O^{3+} + Cl^- \quad (9)$$
$$[M]_{589} = \qquad\qquad [M]_{589} =$$
$$5500° \qquad\qquad 2280°$$

rate for this process, $k_{H_2O} = (2.22 \pm 0.10) \times 10^{-4}$ s^{-1}, is similar to that for other 2+ ions,[9] but **1-Cl** fails to show any appreciable signs of aquation (<5%); over one day at 25.0 °C, k_{H_2O} < 10^{-6} s^{-1}. Both isomers readily undergo Hg^{2+}-catalyzed aquation with full retention of configuration and chirality (eq 10 and 11). The method given in eq 10 and 11 proved to be

$$\Lambda\text{-}1\text{-}Cl^{2+} + Hg^{2+} + H_2O \rightarrow \Lambda\text{-}1\text{-}H_2O^{3+} + HgX^+ \quad (10)$$
$$[M]_{589} = \qquad\qquad\qquad [M]_{589} =$$
$$-2450° \qquad\qquad\qquad -2900°$$

$$\Delta\text{-}2\text{-}Cl^{2+} + Hg^{2+} + H_2O \rightarrow \Delta\text{-}2\text{-}H_2O^{3+} + HgX^+ \quad (11)$$
$$[M]_{589} = \qquad\qquad\qquad [M]_{589} =$$
$$5500° \qquad\qquad\qquad 2310°$$

the best for preparing the optically pure aqua and hydroxo ions. The properties of these species (Figures 1, 4, and 6) were used in estimating the products of base hydrolysis and aquation.

Isomerization and Equilibrium Studies. Whereas both **1-OH$_2$** and **2-OH$_2$** are stable over 3 days in aqueous acid (0.5

Table VI

	angle at		
	A···B,	calcd	
A–H···B	Å	H, deg	symmetry opn
H Bonding in Isomer 1			
N(1)–H(1)···Cl(2)	3.29	155	$x - 0.5, -y - 0.5, -1 - z$
N(4)–H(13)···O	3.14	151	$x - 0.5, -y - 0.5, -z$
N(5)–H(19)···Cl(2)	3.41	150	$x - 0.5, -y - 0.5, -z$
N(5)–H(20)···Cl(3)	3.25	158	$-1 - x, 0.5 - y, -0.5 - z$
N(6)–H(6)···Cl(2)	3.29	157	$-x, 0.5 + y, -0.5 - z$
N(6)–H(5)···O	2.93	175	$-x, 0.5 + y, -0.5 - z$

Angles Subtended at Water Oxygen Atom, Deg

Cl(3)–O–Cl(3)	109	Cl(3)$_a$–O–N(6)	117
Cl(3)$_a$–O–N(4)	91	Cl(3)$_b$–O–N(6)	103
Cl(3)$_b$–O–N(4)	73	N(4)–O–N(6)	150

Table VII

	angle at		
	A···B,	calcd	
A–H···B	Å	H, deg	symmetry opn
H Bonding in Isomer 2			
N(1)–H(2)···Cl(2)	3.26	136	$x, 1 - y, 0.5 + z$
N(1)–H(1)···Cl(4)	3.37	135	$0.5 + x, 1.5 - y, 0.5 + z$
N(3)–H(11)···Cl(2)	3.33	142	$x - 0.5, 0.5 + y, z$
N(3)–H(12)···Cl(3)	3.36	123	$x - 0.5, y - 0.5, z$
N(4)–H(14)···Cl(5)	3.28	157	$x, 2 - y, 0.5 + z$
N(4)–H(13)···Cl(4)	3.43	139	
N(5)–H(14)···Cl(3)	3.46	113	$x - 1, 1 - y, 0.5 + z$
N(5)–H(20)···Cl(5)	3.32	169	$x - 1, 1 - y, 0.5 + z$
N(6)–H(6)···Cl(2)	3.28	100	$0.5 + x, 0.5 + y, z$
N(6)–H(6)···Cl(4)	3.31	156	$0.5 + x, y - 0.5, z$

Angles Subtended at Nitrogen Atoms, Deg

Cl(2)···N(1)···Cl(4)	80	Cl(2)···N(3)···Cl(3)	68
Cl(4)···N(4)···Cl(5)	98	Cl(3)···N(5)···Cl(5)	66
Cl(2)···N(6)···Cl(4)	68		

mol dm^{-3} HClO$_4$, $\mu = 1.0$ (NaClO$_4$)) and a similar property holds for **2-OH** at pH ~9, **1-OH** isomerizes completely to **2-OH** (pH ~9) at a rate of 1.0×10^{-5} s^{-1} at 25 °C.

In the presence of activated charcoal both **1-OH$_2$** and **1-OH** isomerize to **2-OH$_2$** or **2-OH** at room temperature on standing overnight. No **1-OH** (<5%) was found by ion-exchange analysis, and the products after anation with HCl gave only **2-Cl**$^{2+}$. Thus, at least for the aqua and hydroxo species, the "planar" condition of the amidine tridentate is the thermodynamically favored configuration.

Crystal Structures of 1-Cl and 2-Cl. Figure 2 shows the structure of the Λ(–)$_{589}$-[Co(en)(amidine)Cl]$^{2+}$ cation, Λ-**1-Cl**, and Figure 7 the structure of the "planar" cation, **2-Cl**. The latter was established with use of a racemic crystal.

Both structures consist of independent complex cations and anions bound together by an extensive network of hydrogen bonds (Tables VI and VII). Bond lengths, bond angles, and dihedral angles are listed in Tables VIII and IX; atoms are labeled identically. The cobalt atoms are coordinated octahedrally by one ethylenediamine, one chlorine atom, and the tridentate amidine ligand of two different configurations. No structural trans effect to the bound chlorine is evident. However, there is a consistent shortening of the Co–N(2) bond lengths of 0.05 Å compared with the normal lengths (1.95–1.96 Å) found here and in other Co(III) complexes.[17–19] Minor distortions in the angles subtended at cobalt result from

(17) G. J. Gainsford, W. G. Jackson, and A. M. Sargeson, *J. Am. Chem. Soc.*, **101**, 3967 (1979).
(18) I. I. Creaser, S. F. Dyke, A. M. Sargeson, and P. A. Tucker, *J. Chem. Soc., Chem. Commun.*, 289 (1978).
(19) J. Springborg, R. J. Geue, A. M. Sargeson, D. Taylor, and M. R. Snow, *J. Chem. Soc., Chem. Commun.*, 647 (1978): (a) complex **4**; (b) complex **6**.

Table VIII. Bond Lengths (A) and Angles (Deg) for Isomers 1 and 2

Distances

atoms	1	2	atoms	1	2
Co–Cl(1)	2.239 (2)	2.274 (5)	Co–N(1)	1.945 (4)	1.969 (12)
Co–N(2)	1.898 (5)	1.874 (12)	Co–N(3)	1.961 (5)	1.982 (13)
Co–N(4)	1.981 (5)	1.952 (13)	Co–N(5)	1.957 (5)	1.950 (13)
N(1)–C(1)	1.490 (7)	1.489 (19)	N(2)–C(2)	1.302 (7)	1.295 (17)
N(2)–C(3)	1.478 (7)	1.480 (21)	N(3)–C(4)	1.511 (8)	1.480 (20)
N(4)–C(5)	1.483 (8)	1.478 (19)	N(5)–C(6)	1.481 (8)	1.530 (19)
N(6)–C(2)	1.316 (8)	1.338 (18)	C(1)–C(2)	1.505 (7)	1.505 (22)
C(3)–C(4)	1.520 (9)	1.497 (22)	C(5)–C(6)	1.502 (10)	1.497 (21)

Angles

atoms	1	2	atoms	1	2
Cl(1)–Co–N(1)	91.6 (1)	89.6 (4)	Cl(1)–Co–N(2)	170.9 (1)	91.6 (4)
Cl(1)–Co–N(3)	90.5 (1)	88.5 (4)	Cl(1)–Co–N(4)	89.6 (2)	173.9 (4)
Cl(1)–Co–N(5)	91.1 (1)	88.9 (4)	N(1)–Co–N(2)	83.3 (2)	83.9 (5)
N(1)–Co–N(3)	97.2 (2)	168.8 (5)	N(1)–Co–N(4)	173.1 (2)	92.3 (5)
N(1)–Co–N(5)	88.5 (2)	94.9 (5)	N(2)–Co–N(3)	82.8 (2)	85.1 (5)
N(2)–Co–N(4)	96.5 (2)	94.4 (5)	N(2)–Co–N(5)	95.2 (2)	178.7 (6)
N(3)–Co–N(4)	89.6 (2)	90.7 (5)	N(3)–Co–N(5)	173.6 (2)	96.1 (5)
N(4)–Co–N(5)	84.7 (2)	85.2 (5)	Co–N(1)–C(1)	108.1 (3)	110 (1)
Co–N(2)–C(2)	116.4 (4)	118 (1)	Co–N(2)–C(3)	112.2 (3)	115 (1)
C(2)–N(2)–C(3)	118.9 (5)	126 (1)	Co–N(3)–C(4)	112.0 (4)	107 (1)
Co–N(4)–C(5)	107.9 (4)	110 (1)	Co–N(5)–C(6)	111.1 (4)	111 (1)
N(1)–C(1)–C(2)	105.9 (4)	108 (1)	N(2)–C(2)–N(6)	126.9 (5)	125 (-)
N(2)–C(2)–C(1)	114.1 (5)	115 (1)	N(6)–C(2)–C(1)	119.0 (5)	120 (1)
N(2)–C(3)–C(4)	103.7 (5)	105 (1)	N(3)–C(4)–C(3)	109.5 (5)	109 (1)
N(4)–C(5)–C(6)	106.7 (5)	107 (1)	N(5)–C(6)–C(5)	106.4 (5)	106 (1)

Angles (Deg) and Distances (A) in the ZnCl₄²⁻ Anion of Isomer 2

Zn–Cl(2)	2.289 (5)	Zn–Cl(3)	2.223 (5)
Zn–Cl(4)	2.276 (4)	Zn–Cl(5)	2.290 (4)
Cl(2)–Zn–Cl(3)	111.2 (2)	Cl(2)–Zn–Cl(4)	108.2 (2)
Cl(2)–Zn–Cl(5)	108.3 (2)	Cl(3)–Zn–Cl(4)	109.8 (2)
Cl(3)–Zn–Cl(5)	109.9 (2)	Cl(4)–Zn–Cl(5)	109.4 (2)

Table IX. Selected Dihedral Angles (Deg) in Isomers 1 and 2

	1	2		1	2		1	2
CO–N(1)–C(1)–C(2)	36.6	-22.8	N(1)–C(1)–C(2)–N(2)	-30.9	21.8	Co–N(3)–C(4)–C(30	14.7	40.2
Co–N(2)–C(2)–C(1)	10.1	-10.2	N(2)–C(3)–C(4)–N(3)	-38.3	-45.5	Co–N(5)–C(6)–C(5)	35.5	32.1
C(3)–N(2)–C(2)–C(1)	149.3	177.4	Co–N(2)–C(2)–N(6)	-168.6	169.9	N(1)–C(1)–C(2)–N(6)	147.9	-158.4
C(2)–N(2)–C(3)–C(4)	-92.4	-156.6	C(3)–N(2)–C(2)–N(6)	-29.3	-2.4	N(4)–C(5)–C(6)–N(5)	-51.6	-48.1
Co–N(4)–C(5)–C(6)	44.2	43.5	Co–N(2)–C(3)–C(4)	48.4	30.9			

Table X. Bond Lengths (A) in Compounds with Bound Imine and Amidine Ligands^a

Co–N(2)	N(2)–C(2)	C(2)–N(6)	N(2)–C(3)	ref
1.989 (5)	1.302 (7)	1.316 (8)	1.478 (7)	this work
1.874 (12)	1.295 (17)	1.338 (18)	1.480 (21)	this work
1.96 (1)	1.29 (2)	1.32 (3)	1.49 (2)	17
(1.93)	1.295 (6)	1.334 (6)		18
1.90 (1)	1.31 (1)	1.34 (1)		19a
1.88 (1)	1.29 (1)	1.34 (1)		19b
1.924 95)	1.252 (7)			20
1.933 (7)	1.293 (8)			21

a See Figure 2.

Table XI. Minimum Strain Energies (kcal mol⁻¹) for [Co(en)(amidine)Cl]²⁺ Isomers

energy type	1-Cl	1-Cl (cryst)	2-Cl	3-Cl(A)	3-Cl(B)
bond length	0.7	1.5	0.8	0.8	0.8
bond angle	4.7	8.3	3.8	4.5	5.1
nonbonded	-3.8	0.1	-3.2	-1.8	-2.3
(nonbonded^a)	(3.3)	(6.6)	(3.8)	(4.8)	(4.4)
torsional	6.3	5.6	8.8	8.3	6.5
Δ (out of plane)	4.5	4.7	0.1	2.9	4.2
total strain energy	12.3	20.2	10.3	14.8	14.2
differences (based on 2-Cl)	2.0	9.9	0	4.5	3.9

a Interactions restricted to closest contacts (1.16 × Σ(van der Waals radii)).

Table XII. Additional^a Potential Function Parameters for Strain Energy Minimization of [Co(en)(amidine)Cl]²⁺ Isomers

energy type	force const^b	description	"unstrained" value
bond def	9.0	C=N(amidine)	1.32 A
	1.75^d	C–N	1.49 A
	9.0	C=O	1.22 A
	1.41	Co–Cl	2.23 A
angle def	1.0	X–N(amidine)–C	120°
	0.53	H–N(amidine)–H	120°
	0.4^c	Co–N–C	109.3°
torsional def	0.07	C–N(amidine)	0°, 180° (2-fold)
	0.011^c	C–N	60, 120° (3-fold)
	0.017^c	C–C	60, 120° (3-fold)
Δ def	1.0	N(6)–C(2) constrained to N(2), C(1), C(2)	0°
	1.0	N(2)–Co constrained to Co, C(2), C(3)	0°
	1.0	N(2)–C(3) constrained to Co, C(2), C(3)	0°
	1.0	N(2)–C(2) constrained to Co, C(2), C(3)	0°

a Compared with those of previous systems.[21] b Units are 10⁵ dyn cm⁻¹ molecule⁻¹, 10⁻¹¹ erg rad⁻² molecule⁻¹, and 10⁻¹¹ erg molecule⁻¹, respectively. c Values from ref 21 for comparison.

constraints imposed by the amidine ligand.

Bond distances and angles of the amidine moiety are similar in the two isomers and agree with those found in analogous

Table XVIII. Data for the X-ray Diffraction
Study of 1-Cl-Cl·H₂O

(A) Crystal Data at 21 (1) °C

cryst syst: orthorhombic	formula wt = 1438.5
space group: $P2_12_12_1$	ρ(calcd) = 1.588 g cm⁻³
a = 8.473 (3) Å	μ = 140.9 cm⁻¹ (Cu K$\bar{\alpha}$)
b = 12.854 (4) Å	cell constant determination: 12
c = 13.807 (4) Å	high-angle reflections and
V = 1503.7 Å³	refined 2θ, ω, ϕ values in the
Z = 4	range $91 < 2\theta < 119°$ (λ(Cu
cryst habit, size: truncated	Kα_1) 1.540 51 Å)
pyramidal, 8 faces {110},	
{011}; max dimens 0.16 ×	
0.16 × 0.15 mm	

(B) Measurement of Intensity Data

radiation: Cu Kα, graphite crystal monochromator
reflcns measd: hkl (twice), $h\bar{k}l$ (once) to 2θ = 125°
scan type, speed: θ–2θ, 2° min⁻¹
scan range: symmetrical, $[1.7 + \Delta(\alpha_2-\alpha_1)]°$
bkgd measmt: stationary, for 10 s at each of the scan limits
no. of reflcns: 2811, 2204 in "unique" (hkl, $hk\bar{l}$) set
std reflcns: 0,12,0; 066; 405; measd after every 40 reflcns,
showed a steady decrease of 8–16% with time; an isotropic (sin
θ)-dependent correction was applied (see text).

(C) Treatment of Intensity Data^a

abs cor: numerical^b, with use of a grid of 8 × 8 × 8 points
parallel to a, b and c; transmission factors varied from 0.240 to
0.454.
data reduction: intensities, derived structure amplitudes, and esd's
as before^b
statistical information: R_s = 0.030 ($I > 3[\sigma(I)]$)

(D) Refinement^c with 2008 Data for Which $I > 3[\sigma(I)]$

isotropic refinement, all nonhydrogen atoms, correct solution	R = 0.075 (1119 hkl data only)
isotropic refinement, all nonhydrogen atoms, incorrect enantiomer	R = 0.125 (1119 hkl data only)
anisotropic refinement, all non-hydrogen atoms	R = 0.060, R_w = 0.071
anisotropic refinement, H attached to N and C atoms included as fixed contributions	R = 0.049, R_w = 0.051
standard deviation of an observation of unit weight (SDU)	1.961
final difference map	random peaks $\leqslant$ 0.29 e Å⁻³

^{a} $R_s = \Sigma\sigma(|F_o|)/\Sigma|F_o|$. ^{b} Reference 17. ^{c} $R = \Sigma||F_o| - |F_o||/\Sigma|F_o|$, $R_w = [\Sigma w[|F_o| - |F_o|]^2/\Sigma w|F_o|^2]^{1/2}$, SDU = $[\Sigma w[|F_o| - |F_c|]^2/(m-n)]^{1/2}$ where m (=2008) is the number of observations and n (=154) is the number of parameters.

compounds (Table X). C(1), C(2), N(2), and N(6) are strictly coplanar, and there appears to be no obvious constraints imposed on other atoms in the tridentate ligand (Table XVII, supplementary material). The endo N(2)–C(2) and exo C-(2)–N(6) distances are similar in both complexes with mean values of 1.301 (6) and 1.320 (7) Å, respectively. The slightly longer C(2)–N(6) distance is in agreement with that of other compounds (Table X). These C–N values are close to those expected for double bonds (1.26 Å²⁰⁻²²) being considerably shorter than those for single bonds (1.47–1.49 Å¹⁷).

The angles subtended at N(2) and C(2) together with the above bond lengths suggest considerable double-bond character in the N(2)⁓C(2)⁓N(6) grouping. Also the two protons H(5) and H(6) were both located, or resolved, in regions of positive electron density about N(6); no similar indications were found about C(2) or N(2). This is in agreement with the ¹H NMR results (Figure 3). Together with the above bond lengths this suggests considerable N⁓C⁓NH₂⁺ character in agreement with the increased acidity found for 1-X (X = Cl,

Br). Other parameters for the two cations are self-consistent and are in the normal ranges expected for cobalt(III) ethylenediamine compounds, with the same λ conformation in both en rings. It is noteworthy that the Co–N(1)–C(1)–C(2) part of the amidine rings has opposite conformations in the two isomers (see Table IX).

Strain Energy Calculations. The results given in Table XI were obtained with use of a method described previously.²³ Additions to the force field parameters are itemized in Table XII. Final coordinates for the minimized structures are available (Tables XIII–XVI, supplementary material). The calculations confirm the original supposition based on structural models that the planar tridentate 2-Cl configuration is the most stable. Differences lie in lower bond angle and out-of-plane deformation energies. Compared with those of 1-Cl these outweigh increases in both the nonbonded and the torsional energy terms. The most notable nonbonded interaction in 2-Cl is between Cl(1) and H(12) (2.64 Å).

For 3-Cl two stable minima were located corresponding to two conformations of the ethylenediamine ring (ϕ(N(2)–C-(3)–C(4)–N(3)) = 7.8, 46.6°, respectively) (A and B in Table XI). For both structures bond angle and nonbonded and out-of-plane deformations combine to predict them to be less stable than 1-Cl or 2-Cl. Neither was observed at any stage in this study.

The force field parameters are apparently overestimated for the planarity constraints within the amidine ligand as given in Table XVII (supplementary material). By comparison with the crystal values N(1) in 1-Cl and C(4) in 2-Cl appear to have been overconstrained with respect to this plane in the calculations. The satisfactory agreement between all other parameters of the minimized and crystal structures indicates no other major area in which the force field might be improved.

Experimental Section

Analytical reagents were used for kinetic measurements without further purification. Spectrophotometric measurements were made with Cary 14, 16K, or 219 spectrophotometers. Some kinetic data were obtained by using a manually driven stopped-flow device fitted to the Cary 219 spectrophotometer or by using a Durrum-Gibson stopped-flow spectrophotometer. Infrared measurements were made with a Perkin-Elmer 457 spectrophotometer, and optical rotations were recorded on a Perkin-Elmer P22 spectropolarimeter using a 1-dm cell (±0.002°). pH measurements were made with Radiometer equipment,²ᵇ and ¹H NMR spectra were recorded on Varian HA100, JEOL Minimar MH100, or Varian T60 spectrometers with use of collidine/DCl buffers (0.010, 0.009 mol dm⁻³, pD = 6.9).

Preparation of Complexes. *cis*-[Co(en)₂(NH₂CH₂CN)X]X₂ (or (ClO₄)₂) salts (X = Cl, Br) were prepared and resolved into their optical forms as described previously.²ᵇ

For the preparation of complexes containing the [Co(en)(amidine)X]²⁺ (isomer 1) ions, *cis*-[Co(en)₂(NH₂CH₂CN)X]X₂ (3.0 g) in water at pH 8.5 (20 cm³, 0.05 mol dm⁻³ Tris buffer) was allowed to stand at room temperature for 5 min. Hydrochloric acid (or HBr) was added (1 cm³ of the concentrated acid), the solution filtered, and LiClO₄ added (6–10 g). When the mixture was cooled to 0 °C, purple-red crystals of [Co(en)(amidine)X](ClO₄)₂ formed. These were washed with iced MeOH and ether and then air-dried. Anal. Calcd for [Co(en)(amidine)Cl](ClO₄)₂: C, 15.35; H, 4.29; N, 17.90. Found: C, 15.6; H, 4.2; N, 17.9. Calcd for [Co(en)(amidine)-Br](ClO₄)₂: C, 14.02; H, 3.92; N,, 16.35. Found: C, 14.1; H, 4.0; N, 16.4. Alternatively, following acidification, addition of LiCl or LiBr resulted in the chloro or bromo salts. These were recrystallized from warm water by cooling and adding HCl or HBr. Anal. Calcd for [Co(en)(amidine)Cl]Cl₂·H₂O: C, 20.05; H, 6.13; N, 23.37; Cl, 29.58. Found: C, 20.1; H, 6.3; N, 23.1; Cl, 29.5. Calcd for [Co-(en)(amidine)Br]Br₂·H₂O: C, 14.62; H, 4.50; N, 17.05. Found: C, 14.6; H, 4.6; N, 17.0. Molar absorptivities of the chloro and bromo ions were ϵ_{552} 222, ϵ_{567} 279 (1 mol dm⁻³ NaClO₄, pH 2).

(20) G. B. Robertson and P. O. Whimp, *Aust. J. Chem.*, **28**, 729 (1975).
(21) G. B. Robertson and P. O. Whimp, *Aust. J. Chem.*, **28**, 2129 (1975).
(22) A. Monaci, F. Tarli, A. M. M. Lanfredi, A. Tiripicchio, and M. T. Camellini, *J. Chem. Soc., Dalton Trans.*, 1436 (1979).

(23) D. A. Buckingham, P. J. Cresswell, R. J. Dellaca, M. Dwyer, G. C. Gainsford, L. G. Marzilli, I. E. Maxwell, W. T. Robinson, A. M. Sargeson, and K. R. Turnbull, *J. Am. Chem. Soc.*, **96**, 1713 (1974).

Table XIX. Data for the X-ray Diffraction Study of 2-Cl-ZnCl₄

(A) Crystal Data at 18 (2) °C

cryst syst: monoclinic
space group: *Cc*
$a = 10.405\ (3)$ Å
$b = 11.858\ (3)$ Å
$c = 14.104\ (6)$ Å
$V = 1733.2$ Å³
$Z = 4$
cryst habit, size: triangular prism,
  6 faces {0,1,0} (1,0,0), {0,0,0},
  and (−1,0,1); max dimens 0.16 ×
  0.09 × 0.06 mm

formula wt = 1926.0
ρ(calcd) = 1.85 g cm⁻³
ρ(obsd) = 1.85 (2) g cm⁻³
  flotation
μ = 31.8 cm⁻¹ (Mo Kα)
cell constant determination:
  12 high-angle reflections, re-
  fined 2θ, ω, ϕ values in the
  range $27 < 2\theta < 22°$ (λ(Mo
  Kα) 0.710 69 A)

(B) Measurement of Intensity Data

radiation: Mo Kᾱ, Zr filtered
reflcns measd: hkl, $\bar{h}kl$ to $2\theta = 54°$
scan type, scan step: θ–2θ, 1.5s count each 0.01°
scan range: symmetrical, fixed 0.44° (θ 1–45°), 0.54° (θ 45–54°)
bkgd measmt: stationary, for 16.5 s at each of the scan limits
no. of reflcns measd: 2131, 1968 in "unique" set
std reflcns: −2,0,0; 021; 004; measd after every 100 reflcns; only
  random fluctuations of up to ±3% of their mean values over the
  collection.

(C) Treatment of Intensity Data

abs cor: analytical;[31] transmission factors varied from
  0.71 to 0.83
data reduction: intensities, derived structure amplitudes,
  and esd's

(D) Refinement with 1083 Data for Which $I > 3.5\ [\sigma(I)]$

isotropic refinement, all nonhydrogen $R = 0.080$
  atoms preabsorption data
Co, Zn, Cl anisotropic atoms, all other $R = 0.057$
  nonhydrogen atoms isotropic, post-
  absorption data
as above, with hydrogens in calcd riding $R = 0.049$, $R_w = 0.053$
  positions except resolved ones on N(6)
final difference map random peaks around <0.6 e A⁻³
  heavy atoms

Table XX. Atomic Coordinates (×10⁴) and Isotropic Temperature Factors (×10³) for 1-Cl-Cl·H₂O[a]

atom	x	y	z	U_{iso},[b] Å²
Co	5602.7 (10)	8300.95 (66)	6781.34 (63)	23
Cl(1)	4674.1 (20)	6749.8 (12)	6287.5 (12)	43
Cl(2)	9832.7 (18)	6687.1 (13)	6297.0 (10)	41
Cl(3)	5663.3 (23)	6474.1 (11)	9619.3 (12)	49
O	9379.9 (58)	6327.3 (31)	9938.6 (30)	45
N(1)	7016.7 (53)	8386.0 (35)	5674.5 (30)	24
N(2)	6706.2 (55)	9510.2 (35)	7187.1 (30)	22
N(3)	7073.6 (59)	7608.3 (34)	7668.4 (31)	27
N(4)	3990.9 (57)	8325.4 (39)	7820.7 (34)	36
N(5)	4019.7 (58)	9054.6 (35)	6023.9 (34)	30
N(6)	8703.7 (63)	10663.4 (38)	6715.6 (36)	38
C(1)	7488.9 (73)	9494.5 (42)	5548.1 (36)	27
C(2)	7648.6 (73)	9932.5 (44)	6554.3 (38)	26
C(3)	7220.9 (75)	9442.7 (44)	8207.7 (41)	32
C(4)	7994.9 (73)	8378.3 (52)	8272.1 (45)	44
C(5)	2850.2 (81)	9166.0 (54)	7594.3 (49)	51
C(6)	2481.9 (78)	9080.1 (56)	6532.9 (53)	52
H(1)	6458	8132	5073	36
H(2)	7983	7944	5795	36
H(3)	8600	9545	5168	38
H(4)	6596	9914	5149	38
H(5)	9391	1.0922	6168	50
H(6)	8826	1.0965	7387	50
H(7)	8055	1.0051	8377	44
H(8)	6224	9495	8693	44
H(9)	8009	8124	9018	54
H(10)	9191	8426	8004	54
H(11)	7839	7177	7277	39
H(12)	6456	7139	8115	39
H(13)	4512	8467	8465	49
H(14)	3426	7634	7847	49
H(15)	1787	9068	8016	63
H(16)	3365	9916	7751	63
H(17)	1800	9743	6298	64
H(18)	1828	8375	6390	64
H(19)	3881	8697	5378	42
H(20)	4395	9791	5916	42

[a] Standard deviations in the least significant digit appear in parentheses in this and subsequent tables. [b] For atoms refined anisotropically, $U_{iso} = U_{eq} = \frac{1}{3}\Sigma_i\Sigma_j U_{ij}a_i^*a_j^*a_ia_j$; see Table XXI.

Table XXI. Anisotropic Temperature Factors (×10³) for 1-Cl-Cl·H₂O[a]

atom	U_{11}	U_{22}	U_{33}	U_{12}	U_{13}	U_{23}
Co	20.6 (4)	23.5 (4)	23.3 (4)	−1.0 (5)	−1.1 (4)	−0.8 (4)
Cl(1)	53 (1)	27.9 (7)	49.1 (9)	−11.2 (9)	−11.8 (8)	−1.9 (8)
Cl(2)	35.8 (9)	56.0 (9)	31.0 (7)	18.2 (9)	6.1 (7)	5.2 (9)
Cl(3)	52 (1)	36.5 (9)	58 (1)	−3.4 (9)	19 (1)	−1.3 (8)
O	48 (3)	45 (3)	42 (3)	12 (3)	0 (3)	−4 (2)
N(1)	28 (3)	27 (3)	18 (2)	5 (2)	−4 (2)	−3 (2)
N(2)	21 (3)	27 (3)	18 (2)	−4 (2)	3 (2)	0 (2)
N(3)	26 (3)	31 (3)	23 (3)	1 (2)	−2 (2)	1 (2)
N(4)	29 (3)	41 (3)	39 (3)	−5 (3)	7 (2)	−1 (3)
N(5)	29 (3)	27 (3)	35 (3)	−4 (3)	−1 (3)	−1 (2)
N(6)	37 (3)	45 (3)	32 (3)	−18 (3)	3 (3)	0 (3)
C(1)	37 (4)	32 (3)	13 (3)	0 (3)	1 (3)	0 (2)
C(2)	24 (3)	28 (3)	27 (3)	−5 (3)	−4 (3)	−4 (3)
C(3)	42 (4)	35 (3)	19 (3)	−7 (3)	0 (3)	1 (3)
C(4)	39 (4)	49 (4)	34 (3)	−3 (4)	−9 (3)	1 (4)
C(5)	30 (4)	62 (5)	61 (5)	4 (4)	10 (4)	−1 (4)
C(6)	19 (4)	65 (5)	72 (5)	12 (4)	3 (4)	15 (4)

[a] The form of the thermal ellipsoid is $\exp(-2\pi^2(a^{*2}U_{11}h^2 + ... + 2b^*c^*U_{23}kl + ...)$.

The [Co(en)(amidine)Cl]²⁺ ion (isomer **1**) was resolved into its optical forms as follows. Sodium (+)-arsenyltartrate (1.5 g) was added to a solution of the chloride salt (1.8 g) in water (15 cm³, pH 3, HOAc) at 40 °C. The diastereoisomer was induced to crystallize by scratching with a glass rod as the solution cooled slowly to 20 °C (1.4 g). The filtrate was treated with 12 mol dm⁻³ HCl (0.5 cm³) and cooled, whereupon the chloride salt crystallized. More was obtained by adding HCl (0.5 mL, 12 mol dm⁻³) and cooling over 12 h at 4 °C. The diastereoisomer (0.8 g) dissolved in water (10 cm³, pH 3) was treated with HCl (1 cm³, 12 mol dm⁻³). When the solution was cooled and the container scratched, (−)₅₈₉-[Co(en)(amidine)Cl]Cl₂ was induced to crystallize. This material was recrystallized from water by adding HCl (12 mol dm⁻³) and cooling. Anal. Found: C, 20.2; H, 6.2; N, 23.1; Cl, 29.3. $[M]_{589} = -2450$, $[M]^{25}_{546} = 5200$, and $[M]^{25}_{436} = 5100°$ mol⁻¹ cm dm for a 6.8×10^{-4} mol dm⁻³ solution of the complex in 0.1 mol dm⁻³ HCl. The dextro fractions on recrystallization gave $[M]^{25}_{589} = 2500$, $[M]^{25}_{546} = -5250$, and $[M]^{25}_{436} = -5150°$ mol⁻¹ cm dm under the same conditions.

[Co(en)(amidine)Cl]Cl·ClO₄ (isomer **2**) was prepared as follows. [Co(en)(amidine)Br]Br₂·H₂O (15.0 g, isomer **1**) in water (400 cm³) was base hydrolyzed for 70 min at pH 10.0 under pH stat control. The reaction was quenched by the addition of hydrochloric acid (20 cm³, 5 mol dm⁻³) and the solution evaporated to dryness to give the anated product plus alkali-metal salts. The residual solid was dissolved in water and base hydrolyzed for a further 70 min at pH 10.0 before the reaction was once again quenched by the addition of hydrochloric acid. The aqua products were sorbed onto Dowex 50W-X2 (H⁺ form, 5 × 30 cm), and the column was washed free of salt by elution with 1 mol dm⁻³ hydrochloric acid. Elution with 5 mol dm⁻³ hydrochloric acid removed the products from the column as a single band, which was collected and evaporated to dryness under reduced pressure. The solid was dissolved in the minimum volume of 1% hydrochloric acid and crystallized by the addition of sodium perchlorate. The red-brown product was filtered off, washed with 95% ethanol and then ether, and air-dried (9.6 g). Anal. Calcd for [Co(en)(amidine)Cl]Cl·ClO₄: C, 17.76; H, 4.97; N, 20.72. Found: C, 17.70; H, 5.07; N, 20.3. Molar

absorptivities were ϵ_{548} 116, ϵ_{466} 94 (1 mol dm⁻³ HCl). Alternatively, the chloride salt was crystallized from the concentrated solution by adding methanol and cooling. Anal. Calcd for [Co(en)(amidine)-Cl]Cl₂·H₂O: C, 20.15; H, 6.20; N, 23.51; Cl, 29.75. Found: C, 20.2; H, 6.35; N, 23.4; Cl, 29.6. Addition of ZnCl₂ to a concentrated solution of the chloride salt in hydrochloric acid resulted in the crystallization of flat plates of the tetrachlorozincate salt. Anal. Calcd

Table XXII. Diffraction Data for Crystals of 1-Cl·Cl·H₂O

reflcn	cryst I (data collection cryst) $(F_{hkl}/F_{h\bar{k}l})_{obsd}$	cryst I $(F_{hkl}/F_{h\bar{k}l})_{calcd}$	cryst II (resolved sample) $(F_{h\bar{k}l}/F_{hkl})_{obsd}$
142	0.79	0.82	0.82
143	0.89	0.89	0.89
174	1.14	1.16	1.17
283	1.15	1.14	1.11
284	1.17	1.21	1.13
312	0.81	0.89	0.90
343	1.11	1.14	1.14
411	1.15	1.23	1.20
482	1.09	1.11	1.08
541	0.88	0.91	0.86
542	1.27	1.26	1.21
618	1.11	1.09	1.07
6,1,11	1.10	1.10	1.13
7,1,10	1.28	1.22	1.19
811	1.32	1.31	1.18

for [Co(en)(amidine)Cl](ZnCl₄): C, 15.08; H, 4.22; N, 17.59. Found: C, 15.1; H, 4.1; N, 17.3.

Hydrolysis Products. Isomer 1. Preliminary ion-exchange experiments (Sephadex SP-C25, eluant 0.25 mol dm⁻³ Na₂HPO₄, pH 6.5) showed that base hydrolysis of 1-X (X = Cl, Br) yielded two products, 1-OH (purple-red) and 2-OH (orange) (spectral identification, 650–320 nm, after acidification (aqua)). The pH dependence of the product ratio was calculated from absorbance data at 350 nm following quenching (5 mol dm⁻³ HClO₄) of the reaction mixtures after $(20–30)t_{1/2}$. It was shown that both 1-OH and 2-OH were stable over this time period. However, 1-OH was observed to undergo a slower pH-independent isomerization to give exclusively 2-OH (pH range 8.3–11.2, μ = 1.0 mol dm⁻³ NaClO₄, 25 °C, four experiments) with $k = (1.0 \pm 0.1) \times 10^{-5}$ s⁻¹. Some analyses were carried out by separating 1-OH and 2-OH by ion-exchange chromatography and analyzing the eluted fractions.

Isomer 2. 2-X (X = Cl, Br) was base hydrolyzed (1.0 and 0.1 mol

dm⁻³ NaOH, 25 °C, 30 s and 5 min, respectively) before quenching (5 mol dm⁻³ HClO₄). Comparisons of the visible spectra with authentic 2-OH₂ and 1-OH₂ showed 2-OH₂ to be the only product. Ion-exchange analysis (Sephadex, 0.1 mol dm⁻³ NaClO₄, pH ~9) verified the absence of 1-OH (99.3 and 99.6% recovery).

Aquation of 2-X and 1-X (X = Cl, Br). Solutions of 2-Br quenched after $10t_{1/2}$ and sorbed onto Sephadex SP-C25 resin gave only a single orange band on elution with 0.25 mol dm⁻³ Na₂HPO₄/NaH₂PO₄. This was identical with that produced in the corresponding Hg(II)-induced reaction of 2-X (2-OH₂, ϵ(460 nm) 108.5). Separate experiments with 2-OH₂, and with 1-OH₂ (ϵ(514 nm) 158) produced via the Hg(II)-induced aquation of 1-X, showed that neither underwent measurable isomerization (<5%) over 3 days at 25 °C.

Isomerization on Activated Carbon. Experiments using aqueous solutions of 1-Cl and 2-Cl in the presence of "Norit" activated charcoal (0.5 g) showed that after ca. 12 h at 25 °C both 1-OH₂ (0.1 mol dm⁻³ HClO₄) and 1-OH (0.01 mol dm⁻³ NaOH) had isomerized completely to 2-OH₂ and 2-OH, respectively (visible spectra and chromatography on SP-C25 Sephadex).

Collection and Reduction of Diffraction Data. Isomer 1. Crystals of 1-Cl, [Co(en)(NH₂CH₂CH₂NC(NH₂)CH₂NH₂)Cl]Cl₂·H₂O, were grown as described above. Preliminary Weissenberg and precession photographs indicated an orthorhombic space group, and the systematic absences h00, h = 2n + 1, 0k0, k = 2n + 1, and 00l, l = 2n + 1, led to the unambiguous choice of $P2_12_12_1$. Most operations on the Picker FACS-I diffractometer were carried out as described previously;[24] other operations are described below. Details are given in Table XVIII.

An X-ray-induced decomposition of the crystal necessitated a correction being applied to the raw data. This was done after consideration of the slow, $((\sin\theta)/\lambda)$-dependent decay[25] for (i) the standard reflections and (ii) *pairs* of hkl reflections, for which $I/\sigma(I)$ > 10, in the two *identical* (hkl) octants collected several days apart. The average observed rate constants obtained by these two methods were equal within experimental error, and the intensities were corrected by means of the equation $I_0 = I_t \exp(kt(\sin\theta)/\lambda)$. The equality of the derived rate constants (average $k = 7.70 \times 10^{-3}$ s⁻¹) testifies to the *isotropic* nature of the decomposition, as well as to the appropriateness of this correction for *all* data, not simply the standard reflections. Although applicable to only this data set, the approach

Table XXIII. Final Atomic Coordinates (×10⁴) and Thermal Parameters (×10²) for 2-Cl-ZnCl₄[a]

(1) Anisotropic Atoms

atom	x	y	z	U_{11}[a]	U_{22}	U_{33}	U_{23}	U_{13}	U_{12}
Zn	3460[b]	9810 (2)	4700[b]	2.63 (9)	3.64 (13)	3.52 (12)	0.3 (1)	0.4 (1)	0.0 (1)
Co	2688 (3)	6459 (2)	7499 (2)	2.16 (10)	2.62 (11)	2.47 (12)	0.1 (1)	0.5 (5)	0.3 (1)
Cl(1)	2972 (4)	4694 (4)	8112 (3)	5.16 (28)	3.85 (28)	4.79 (30)	1.3 (2)	1.1 (2)	1.1 (2)
Cl(2)	3718 (4)	11596 (4)	5303 (3)	3.53 (23)	4.15 (27)	3.97 (26)	0.2 (2)	0.6 (2)	−0.3 (2)
Cl(3)	4860 (5)	8620 (4)	5444 (4)	4.74 (25)	4.30 (27)	4.83 (28)	1.2 (2)	0.1 (2)	0.6 (2)
Cl(4)	1409 (4)	9240 (4)	4886 (3)	3.26 (22)	4.97 (28)	4.60 (27)	−0.7 (2)	0.7 (2)	−0.5 (2)
Cl(5)	3760 (5)	9869 (4)	3112 (3)	5.76 (27)	5.66 (30)	3.22 (23)	0.9 (2)	1.5 (2)	2.2 (3)

(2) Isotropic Atoms

atom	x	y	z	U, Å²	atom	x	y	z	U, Å²
N(1)	4141 (12)	6997 (11)	8372 (9)	3.2 (3)	C(1)	5286 (14)	7213 (13)	7837 (12)	3.3 (4)
N(2)	3965 (11)	6225 (10)	6663 (9)	2.8 (3)	C(2)	5137 (14)	6523 (12)	6938 (10)	2.6 (3)
N(3)	1493 (12)	5810 (11)	6468 (9)	3.6 (4)	C(3)	3543 (16)	5587 (15)	5789 (13)	4.4 (5)
N(4)	2275 (12)	7981 (11)	7042 (9)	3.3 (3)	C(4)	2146 (15)	5876 (15)	5579 (12)	4.0 (4)
N(5)	1384 (12)	6727 (11)	8384 (10)	3.6 (3)	C(5)	990 (16)	8314 (16)	7315 (12)	4.5 (5)
N(6)	6171 (12)	6263 (12)	6481 (10)	4.2 (4)	C(6)	919 (15)	7951 (13)	8325 (11)	3.1 (4)

(3) Hydrogen Atoms (Constrained, U = 0.066 (12) Å²)

atom	x	y	z	atom	x	y	z
H(1)	4380	6365	8910	H(11)	606	6289	6392
H(2)	3867	7769	8707	H(12)	1283	4943	6627
H(3)	5338	8098	7663	H(13)	2270	8001	6276
H(4)	6155	6966	8263	H(14)	2993	8562	7352
H(5)	6945	6653	6970	H(15)	874	9218	7258
H(6)	6236	5805	5825	H(16)	244	7903	6859
H(7)	4087	5844	5208	H(17)	1533	8475	8800
H(8)	3663	4692	5907	H(18)	−63	8005	8514
H(9)	1703	5287	5065	H(19)	1794	6553	9100
H(10)	2059	6721	5294	H(20)	574	6173	8209

[a] The form of the thermal ellipsoid is $\exp(-2n^2(a^{*2}U_{11}h^2 + ... + 2b^*c^*U_{23}kl + ...))$. [b] Fixed; see text.

used would appear to be more thorough than other methods[26] provided sufficient data are available. If necessary such data could be generated at the conclusion of the collection.

Isomer 2. Crystals of racemic 2-Cl-ZnCl$_4$ were grown as given above, and by the same methods the systematic absences *hkl*, *h + k* = 2*n* + 1, and *h0l*, *l* = 2*n* + 1, were established, leading to the monoclinic space groups *Cc* or *C2/c*. Standard operations were carried out on a Hilger and Watts Y290 diffractometer controlled by a PDP8/I computer.[23] Details of the analysis are given in Table XIX.

Solution and Refinement. Isomer 1. The structure was solved and refined by conventional Patterson, difference Fourier, and least-squares techniques.[24] Hydrogen atoms were included as fixed contributions to F_c (r_{N-H} = 1.01 Å, r_{CH} = 1.08 Å) in the final cycles of least-squares refinement;[27] the calculation procedure was repeated after each cycle. In the final cycle, no individual parameter shift was greater than 0.13 of the corresponding estimated standard deviation (esd). A weighting-scheme analysis revealed no serious dependence of $w[|R_o| - |F_c|]^2$ on either $|F_o|$ or (sin θ)/λ. Final atomic coordinates and thermal parameters, U_{ij}, together with their estimated standard deviations, are listed in Tables XX and XXI. Tables of observed and calculated structure factor amplitudes are available (see supplementary material).

The absolute configuration of 1-Cl was established by least-squares refinement of the coordinates of both enantiomers, with isotropic temperature factors (Table XVIII); inspection of the final $|F_o|$ vs. $|F_c|$ table, which contains both *hkl* and *h$\bar{k}$l* data, supports this choice. Since the crystal was selected from a racemic mixture, it was not possible to correlate the RD spectrum of the resolved species with the absolute configuration. Hence a crystal of optically pure 1-Cl, $\Delta(+)_{589}$-[Co(en)(amidine)Cl]Cl$_2$·H$_2$O ([M]$_{589}$ = 2500° cm dm mol^{-1}), was mounted and a partial data set, *hkl* and *h$\bar{k}$l*, obtained. Inspection of Table XXII reveals that the absolute configuration of this crystal is enantiomeric with respect to the crystal selected from the racemic mixture. The crystal used in the structure determination therefore contains the $\Lambda(-)_{589}$ enantiomer.

Isomer 2. The structure was solved by direct methods and difference Fourier function calculations. Full-matrix least-squares refinements[28] were carried out with a minimization of $\sum w(|F_o| - |F_c|)^2$. The atomic scattering factors for nonhydrogen atoms were taken from the usual tabulation[29] and those for hydrogen from Stewart.[30] Both *x* and *z* coordinates of the Zn atom were fixed. One of the two hydrogen atoms on N(6) was resolved and the other calculated. The remaining hydrogen atoms were included in calculated positions, with refinement of them as riding atoms[28] (d(N–H), d(C–H) = 1.08 Å; H–X–H = 109.5°), with one common isotropic temperature factor. No individual parameter shift was greater than 0.05 of the corresponding esd in the final cycle. Average values of the minimized function showed little dependence on either $|F_o|$ or (sin θ)/λ.

Final atomic coordinates and thermal parameters, together with their esds, are listed in Table XXIII. Listings of observed and calculated structure factors are available as supplementary material.

(24) B. M. Foxman, *Inorg. Chem.*, **17**, 1932 (1978).
(25) A. L. Beauchamp, M. J. Bennett, and F. A. Cotton, *J. Am. Chem. Soc.*, **90**, 6675 (1969).
(26) J. A. Ibers, *Acta Crystallogr.*, Sect. B, **B25**, 1667 (1969).
(27) Since it was thought that the positions would be used to calculate the magnitude of nonbonded interactions, the spectroscopic values were used rather than more appropriate values: M. R. Churchill, *Inorg. Chem.*, **12**, 1213 (1973).

(28) G. M. Sheldrick, "SHELX, a Programme for Crystal Structure Determination", University of Cambridge, Cambridge, England, 1977.
(29) "International Tables for X-ray Crystallography", Vol. IV, Kynoch Press, Birmingham, England, 1974.
(30) R. F. Stewart, E. R. Davidson, and W. T. Simpson, *J. Chem. Phys.*, **42**, 3175 (1965).
(31) J. De Meulenaer and H. Tompa, *Acta Crystallogr.*, **19**, 1014 (1965).